NASA-TM-86285 19840022497

NASA Technical Memorandum 86285

STRATOSPHERIC NO AND NO_2 PROFILES AT SUNSET FROM ANALYSIS OF HIGH-RESOLUTION BALLOON-BORNE INFRARED SOLAR ABSORPTION SPECTRA OBTAINED AT $33^{o}N$ AND CALCULATIONS WITH A TIME-DEPENDENT PHOTOCHEMICAL MODEL

C. P. Rinsland, R. E. Boughner, J. C. Larsen, A. Goldman,
F. J. Murcray, and D. G. Murcray

AUGUST 1984

National Aeronautics and
Space Administration

Langley Research Center
Hampton, Virginia 23665

Summary

Stratospheric infrared solar absorption spectra recorded in the 1300-2000-cm^{-1} region have ben analyzed to derive simultaneous sunset profiles of NO and NO_2. The spectral data were obtained at sunset with the 0.02-cm^{-1} resolution University of Denver interferometer system during a balloon flight from Alamogordo, New Mexico, near 33° N on October 10, 1979. The technique of nonlinear least squares spectral curve fitting has been used to analyze the stratospheric spectra in regions of absorption by NO and NO_2 lines. To correct for the rapid diurnal changes in NO and NO_2 concen-trations near sunset, a grid of time-dependent altitude profiles has been calculated for both gases with a detailed photochemical model. From these values, normalized diurnal correction factors have been derived for each scan and have been incorporated into the onion-peeling inversion procedure. The retrieved NO and NO_2 profiles are compared to previously published remote infrared and in situ measurements. The CO_2 profile was also determined from the analysis of the NO spectral region and is presented.

1. Introduction

Retrievals of the stratospheric gas concentration profiles of NO and NO_2 from spectra recorded in the solar occultation mode are complicated by rapid changes at twilight which cause the concentration to be a function of solar zenith angle as well as altitude. Photochemical model calculations have shown that large errors in inferred NO concentration in the lower stratosphere will result at sunrise and sunset if this effect is neglected in the inversion procedure [Murcray et al., 1978; Boughner et al., 1980]. The magnitude of the error increases with decreasing altitude and can exceed 100 percent for NO near 25 km [Boughner et al., 1980]. For NO_2, the changes in concentration during sunrise and sunset are of a smaller magnitude, but the corresponding errors still amount to several percent in the lower stratosphere [Kerr et al., 1977; Murcray et al., 1978; Larsen and Boughner, 1981].

Although in situ techniques avoid this problem and have been used to measure stratospheric concentrations of NO and NO_2 [cf. Patel et al., 1974; Maier et al., 1978; Mihelcic et al., 1978; Horvath et al., 1983], solar absorption measurements are important because the simultaneous profiles of a large number of related species (e.g. H_2O, CH_4, O_3, HNO_3, N_2O) can be obtained frequently from the same data set [cf. Goldman et al., 1980; Louisnard et al., 1983] in addition to pressure and temperature [Toth, 1977; Park, 1982; Rinsland et al., 1983a]. Shortly, satellite solar occultation measurements of NO and NO_2 (as well as other species) will be made on a global scale by the Halogen Occultation Experiment [Russell et al., 1977] and by the Atmospheric Trace Molecule Spectroscopy (ATMOS) experiment [Morse, 1980]. It is important, therefore, to develop techniques for

improving the accuracies of NO and NO_2 inversions from solar absorption data.

Boughner et al. [1980] have described a procedure for the calculation of normalized factors which can be incorporated into an onion-peeling retrieval to correct for diurnal changes during a solar occultation event. These factors are derived from time-dependent altitude profiles calculated with a photochemical model and express the variation in concentration with solar angle at a fixed altitude in terms of the 90° (tangent point) concentration. By normalizing, the need to know the absolute level of the profile is removed and instead it is determined from the retrieval process. Blatherwick et al. [1980] used this approach to derive a preliminary NO sunset profile from measurements of the equivalent widths of three isolated NO lines in solar absorption spectra recorded with the University of Denver balloon-borne interferometer system. In these calculations, the diurnal correction factors were estimated from NO distributions obtained with a relatively simple photochemical model [Murcray et al., 1978]. The starting profiles for the photochemical calculations were taken from values in the literature, and a standard atmosphere pressure-temperature profile was assumed in both the photochemical calculations and in the retrieval analysis.

Although the diurnal model and the equivalent width method employed by Blatherwick et al. [1980] represent a reasonable and simple technique to obtain a first approximation to the NO sunset profile, it is important to know if further refinements in the photochemical calculations and in the analysis of the spectroscopic data would yield a significant improvement in the accuracy of the results for NO. For this reason, we have undertaken a reanalysis of the same set of University of Denver stratospheric spectra.

In addition to NO, the profile of NO_2 has also been retrieved. The detailed photochemical model of Callis et al. [1983] has been used to calculate time-varying altitude profiles for both gases. These profiles have been integrated along the refracted ray to determine normalized diurnal correction factors for each of the spectra. To match the experimental conditions as close as possible, the profiles of related trace species obtained from the analysis of the same data set and correlative measurement of pressure and temperature have been used as inputs to these photochemical calculations. The stratospheric spectra have been analyzed with the technique of nonlinear least squares spectral curve fitting [cf. Chang et al., 1978; Niple, 1980; Park, 1983]. Although the reliability of this technique has yet to be studied in detail, it should at least in principle be more accurate than the equivalent width method because of its more complete use of the available information. An iterative photochemical model calculation/spectral inversion procedure has been adopted so that the NO and NO_2 profiles obtained from the analysis are consistent with the retrieval results. The final sunset NO and NO_2 profiles obtained from the analysis are compared with the previous values derived from the same set of spectra [Blatherwick et al., 1980; Niple et al., 1980] and with other published infrared and in situ measurements.

In addition, the profile of CO_2 has been derived from the analysis of the NO spectral region. Since there is considerable evidence that the CO_2 mixing ratio is about 325 ppmv in the mid-stratosphere [cf. Volz et al., 1981], the retrieval of the simultaneous CO_2 profile provides a check for systematic errors in the inversion procedure.

Research at Systems and Applied Sciences Corporation was supported by NASA. Research at the University of Denver was supported by NASA and NSF. We thank R. A. Toth of JPL for sending us calculated line parameters for the

6.2 μm NO_2 bands prior to publication. P. L. Rinsland of NASA Langley Research Center developed some of the programs used in the analysis.

2. Photochemical Calculations

A detailed time-dependent photochemical model [Callis et al., 1983] which incorporates all chemical reactions involving the HO_x, Cl_x, NO_x, and O_x families known to be important was used to calculate time-varying altitude profiles of NO and NO_2 for specified input distributions of temperature, pressure, and the long-lived species such as O_3, H_2O, CH_4, N_2O, and HNO_3. Photolysis rates include single scattering, calculated numerically for a spherical atmosphere. Reflection of direct solar radiation from the surface and clouds was approximated with a surface albedo of 30 percent.

Correction factors derived from two sets of photochemical calculations were used in the analysis. The initial calculation (case A) took profiles of the long-lived species obtained from a steady-state version of the photochemical model and temperature and pressure values from the 1976 U.S. Standard Atmosphere. The analysis of the spectral data with these factors provided a preliminary set of NO and NO_2 profiles for the second set of calculations (case B). Values for N_2O_5 consistent with these NO and NO_2 profiles were inferred from an approximate iterative scheme that equated the increase in N_2O_5 at night to its daytime loss by photolysis. The equations describing the variations of N_2O_5 at night allowed for the conversion of NO_2 into N_2O_5, via NO_3, and into $ClONO_2$. A Cl_x mixing ratio which becomes asymptotic to 2 ppbv in the upper stratosphere was adopted. Initially, no N_2O_5 was assumed to be present at sunset. This amount was increased and adjusted iteratively until the calculated NO_x ($NO+NO_2$) concentrations at sunset matched the case A values.

Profiles of H_2O, CH_4, O_3, HNO_3, and N_2O obtained from the same data set [Goldman et al., 1980, Rinsland et al., 1982a; Rinsland et al., 1984a] and correlative radiosonde and global satellite measurements of temperature and pressure (M. Gelman, National Meteorological Center, private communication, 1981) were also used in the revised (case B) calculations. The diurnal calculations were made for solar zenith angles corresponding to the date and latitude of the measurements and were run for 2-1/2 days, starting at local noon, which was sufficient for the short-lived species to adjust to the concentrations of the long-lived species. After this time, the diurnal profiles were found to be reproducible to $\approx$ 10 percent. Time steps were adjusted to limit truncation errors and ranged from microseconds near sunrise and sunset to $\approx$ 1 hour near noon and midnight. Model calculated values of NO and NO_2 for case B agreed within 20-30 percent with the initial profiles (case A) retrieved for these species.

3. Diurnal Correction Factors

We next discuss the definition of the path-averaged diurnal correction factors used in the analysis. The geometry of a solar occultation event is shown schematically in figure 1 for three atmospheric paths with solar zenith angles θ_0, θ_1, and θ_2. The nomenclature presented here follows that used by Goldman and Saunders [1979]. Ray 0 corresponds to the atmospheric path for a spectrum recorded prior to local sunset ($\theta_0<90°$); rays 1 and 2 trace the paths for two successive low Sun scans with tangent altitudes Z_1 and Z_2 respectively. In our example, the layer boundaries are defined by

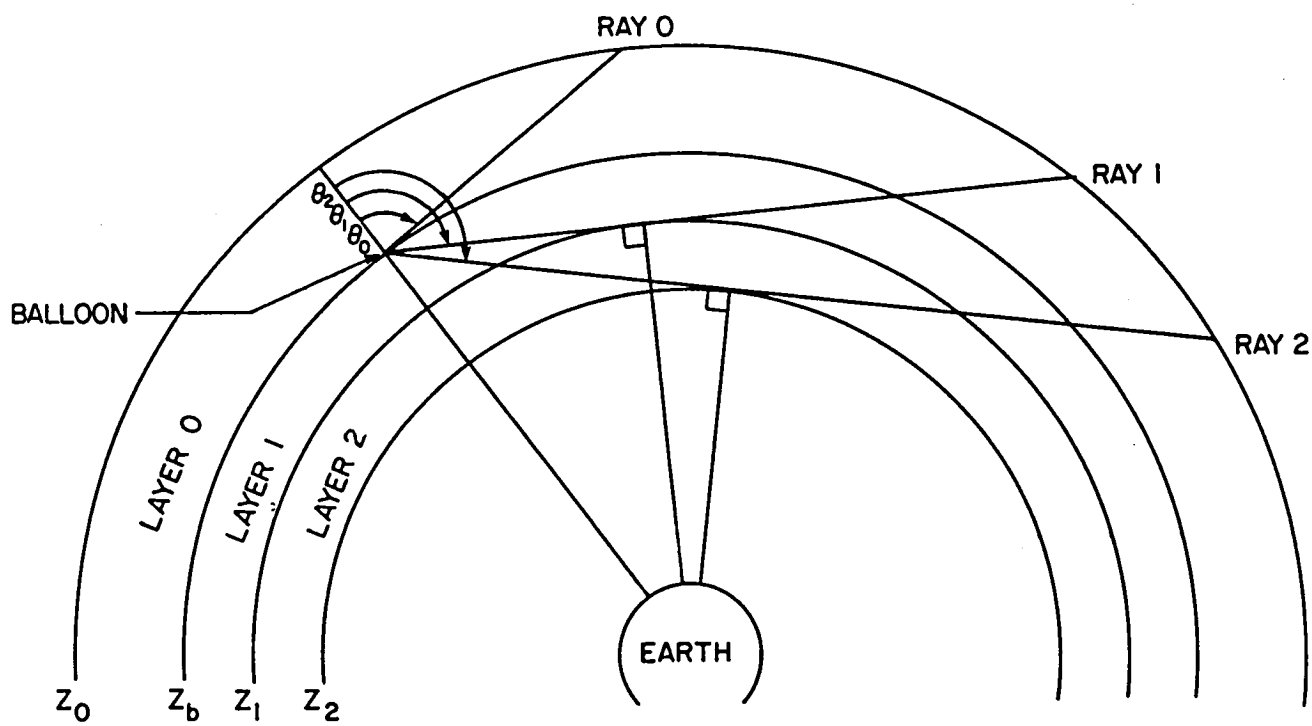

Fig. 1. Solar ray paths for occultation measurements obtained from float altitude Z_b for high Sun (ray 0) and low Sun (rays 1 and 2) cases. The tangent altitudes of the low Sun scans are Z_1 and Z_2, respectively. The upper boundary of the atmosphere is Z_0.

the top of the atmosphere Z_0, the balloon float altitude Z_b, and the tangent altitudes of the two low Sun scans. For simplicity, only a single layer has been shown for the range of altitudes above the balloon so that ray i passes through layer 0 and i inner layers.

The infinite resolution transmittance of the atmosphere at frequency ν corresponding to absorption by a gas along path i across layer 0 and i inner layers has been approximated by

$$T_\nu(i) = \exp \left\{ - \sum_{j=0}^{i} \left[- k_\nu(j)\, U(i,j) \right] \right\} \qquad (1)$$

where k_ν is the monochromatic absorption coefficient (cm^2/molecule) at ν in layer j and U(i,j) is the total absorber amount (molecules/cm^2) along path i across layer j. The values of k_ν are calculated from the positions, intensities, air-broadened halfwidths, and lower state energies of lines of the absorbing gas, assuming a Voigt line shape and the mass-weighted effective pressure and effective temperature for the path through the layer. The column amount is obtained from the integration of density along the refracted ray,

$$U(i,j) = \int_{\substack{\text{path } i \\ \text{layer } j}} \rho(z,\theta)\, ds(z,\theta) \qquad (2)$$

where $ds(z,\theta)$ is the path increment, z is the altitude, and θ is the local solar zenith angle.

According to the analysis of Boughner et al. [1980], the quantity U(i,j) can be rewritten as

$$U(i,j) = \int_{\substack{\text{path } i \\ \text{layer } j}} N(z,\theta)\ \rho(z,\ 90°)\ ds(z,\theta) \qquad (3)$$

where $\rho(z,\ 90°)$ is the sunset density distribution of the gas and

$$N(z,\theta) = \rho(z,\theta)/\rho(z,\ 90°) \qquad (4)$$

is the normalized variation of the concentration with zenith angle relative to the sunset value at altitude z. The $N(z,\theta)$ factor is obtained from the time-dependent photochemical calculations. The advantage of using this normalization is that it is not very sensitive to reasonable variations in the photochemical model inputs [Larsen and Boughner, 1981].

The path-averaged diurnal correction factor for path i across layer j, R(i,j), is defined as the ratio of the time-dependent column amount along the path, U(i,j), to the column amount that would be present with the sunset distribution $\rho(z,90°)$,

$$R(i,j) = U(i,j)/U_S(i,j), \qquad (5)$$

where

$$U_S(i,j) = \int_{\substack{\text{path } i \\ \text{layer } j}} \rho(z,\ 90°)\ ds(z,\theta) \qquad (6)$$

If $R(i,j)>1$, the time-dependent column amount along the path is larger than the corresponding sunset column amount; if $R(i,j)<1$, it is smaller. The path-averaged sunset density corresponding to path i through layer j is given by

$$\rho_s(i,j) = U_s(i,j)/S(i,j), \tag{7}$$

where

$$S(i,j) = \int_{\substack{\text{path } i \\ \text{layer } j}} ds(z,\theta) \tag{8}$$

is the total path length of the ray across the layer.

In an onion-peeling inversion, an average density or average mixing ratio is inferred from the retrieved column amount in the tangent layer and then is usually assigned to this same altitude region in the analysis of spectra with successively lower tangent heights. However, if the concentration varies rapidly with altitude, different paths across a layer will correspond to different average densities (or mixing ratios), and this approximation will cause errors in the calculation of the column amounts. To correct for gradients in the concentration within a layer, a second set of normalized factors has been included in the analysis, defined by

$$N(i,j) = \rho_s(i,j)/\rho_s(j,j), \tag{9}$$

where $\rho_s(j,j)$ is the path-averaged sunset density for the case that layer j is the tangent layer. The values of R(i,j) and N(i,j) must be adjusted iteratively so that the $\rho(z,90°)$ distribution used in the calculations is consistent with the shape of the retrieved vertical profile.

From equations (1), (5), (7), (8), and (9), the infinite resolution transmittance at frequency ν corresponding to absorption by a gas along path i across layer 0 and i inner layers is

$$T_\nu(i) = \exp\left[-\sum_{j=0}^{i-1} k_\nu(j)\, R(i,j)\, N(i,j)\, S(i,j)\, \rho_s(j,j) + k_\nu(i)\, R(i,i)\, S(i,i)\, \rho_s(i,i)\right]. \qquad (10)$$

The first term in brackets contains the contribution to the total absorption from layer 0 above the balloon and the (i-1) inner layers above the tangent layer; the second term is the contribution of the absorption from within the tangent layer. For comparison with the solar absorption spectra, the monochromatic transmittances must be convolved with the effective instrument line shape function and scaled to simulate the wavelength dependence of the instrumental response and the solar flux. These instrumental factors have been determined in the nonlinear least squares analysis of the spectral data. The value of $\rho_s(i,i)$, the path-averaged sunset density in the tangent layer, is the only unknown in equation (10) and is also determined in the least-squares analysis.

4. Data and Analysis

The spectral data were acquired at an apodized FWHM resolution of 0.02 cm^{-1} with a Michelson-type Fourier transform interferometer (maximum path difference 50 cm) during a balloon flight from Alamogordo, New Mexico (32.8°N, 106.0°W), on October 10, 1979. Sample stratospheric spectra obtained in both the NO and NO_2 regions have been published in an atlas format with line positions and identifications of the observed atmospheric and solar features [Goldman et al., 1983]. The atlas also contains the same information for additional spectral regions recorded during the 1978 and 1981 University of Denver balloon flights. The identifications given in the present work are taken from this atlas. The signal-to-rms noise is about 100 in the NO and NO_2 regions.

The application of the technique of nonlinear least squares spectral curve fitting to the analysis of University of Denver balloon-borne stratospheric spectra is discussed in several papers [Goldman et al., 1980, Niple, 1980; Niple et al., 1980; Rinsland et al., 1982a; Rinsland et al., 1983a] and, therefore, a description is not repeated here. In the present study, the NO and NO_2 profiles have been derived from six scans recorded at the float altitude of 33.0 ± 0.5 km. The correlative National Meteorological Center pressure-temperature profile assumed in the photochemical model calculations has also been adopted in the ray-tracing calculations with the FASATM program [Gallery et al., 1983]. The National Meteorological Center measurements indicate a tropopause height of 14.9 km. The solar zenith angle corresponding to the time at which the zero path difference of the interferogram is recorded has been shown to be the appropriate effective solar zenith angle for airmass calculations [Park, 1982; Kyle and Blatherwick, 1984] and has been used for each scan in the ray-tracing

calculations. We note that in the previous analyses of NO and NO_2 [Blatherwick et al., 1980; Niple et al., 1980], the mean solar zenith angles were used in the airmass calculations.

Solar CO lines occur in both the NO and NO_2 spectral regions. Their absorption has been simulated with the Minnaert formula [cf., Kilston, 1975], using the method described by Rinsland et al. [1982a]. The molecular constants reported by Guelachvili et al. [1983] were used to calculate the positions of these lines.

4.1 NO Retrieval

The 1903.0-1907.0 cm^{-1} and 1911.95-1917.00 cm^{-1} intervals (464 and 470 data points, respectively) were selected for the analysis. Each region contains four NO lines (actually unresolved lambda doublets separated by 0.011 cm^{-1}), a number of prominent atmospheric absorption lines of CO_2 and H_2O, and numerous lines of solar CO. The NO lines are strongest in the 92.41° and 93.36° scans and are weaker at larger and smaller zenith angles; the CO_2 and H_2O lines strengthen with increasing zenith angle over the entire range of solar zenith angles observed from float altitude (79.2-94.9°). The 93.78° and 94.14° scans also show several weak N_2O lines. No additional species were identified as absorbers within these spectral intervals.

The sunset density of NO and the mixing ratios of CO_2 and H_2O were included as unknowns in the nonlinear least-squares fit to each of the stratospheric spectra. The N_2O profile derived previously from analysis of the same set of stratospheric spectra was assumed [Rinsland et al., 1982a]. Weak channel spectra with periods of 0.24, 0.48, and 1.90 cm^{-1} were observed and modeled with the expressions derived by Niple et al. [1980].

The spectral line parameters were taken mostly from the 1982 Air Force Geophysics Laboratory (AFGL) compilations [Rothman et al., 1983a,b]. These listings include the NO positions and intensities generated recently by Gillis and Goldman [1982] and the water vapor line parameters of Flaud et al. [1981]. Improved CO_2 positions and intensities determined from an analysis of Kitt Peak laboratory spectra [Rinsland et al., 1983b,c; Rinsland et al., 1984b] were assumed. The positions of the stronger H_2O lines were updated to agree with the precise values measured by Guelachvili [1983]. Initial fittings suggested that the intensity of the $H_2{}^{16}O$ line near 1904.761 cm^{-1} ($J'=4$, $K_a'=4$, $K_c'=1 \leftarrow J''=4$, $K_a''=1$, $K_c''=4$) is overestimated in the 1982 AFGL compilation. A revised value was determined by comparison of the relative intensity reported by Guelachvili [1983] for this line on his spectrum 1556 with the relative intensities of several additional stronger and weaker lines for which Toth and Farmer [1975] have reported absolute intensity values. By interpolation, an absolute intensity at room temperature for the 1904.761 cm^{-1} line of $\approx 1.8 \times 10^{-24}$ cm/molecule (64 percent of the 1982 AFGL intensity) has been estimated; with this value, improved least-squares fits were obtained near this line for all spectra. The identified N_2O lines are R-branch transitions from the $\nu_1 + \nu_2{}^1$ band; their positions were taken as reported by Amiot and Guelachvili [1976].

Table I presents the NO densities retrieved with three successive refinements in the analysis. For each set of results, the NO densities obtained from fitting the two spectral intervals agreed to $\approx$ 10 percent and have been averaged. The sunset densities obtained assuming a non-time-dependent (spherically symmetric) NO distribution with constant NO density in a layer (that is $R(i,j) = N(i,j) = 1$, for all paths and layers) are listed to show the results which would be obtained without corrections for diurnal

changes and gradients in the vertical profile. The case A and case B results were calculated with the same set of unknowns in the least-squares spectral analysis and assuming the R(i,j) and N(i,j) factors listed in Table II. Because the shape of the NO profile above the balloon float altitude cannot be determined from the data and has, therefore, been fixed by initial assumption, the average values listed for the layer above the balloon are enclosed in parentheses to indicate their greater uncertainty. An additional iteration of the photochemical model results was not made because, as discussed below, the differences between the case A and case B diurnal correction factors are relatively small and the measured NO profile has a rather large uncertainty, particularly below 25 km.

The R(i,j) factors for cases A and B differ by less than 0.03, despite some rather large differences in the values assumed in the two sets of photochemical calculations. For example, to match the preliminary results for NO (and NO_2), the total odd nitrogen concentrations in the lower stratosphere were increased by nearly an order of magnitude for the case B calculations. The small sensitivity of normalized diurnal correction factors to perturbations in a number of model input parameters has been noted previously [Larsen and Boughner, 1981].

Table III compares the calculated case B diurnal correction factors and the values estimated by Blatherwick et al. [1980]. For the 85.85° and 91.30° scans, the case B results indicate that diurnal corrections are negligibly small, in agreement with Blatherwick et al. [1980]. For the lower Sun scans, the present study yields slightly larger values of R(i,j) for the inner layers above the tangent layer and smaller values for the inner-most (tangent) layer, where Blatherwick et al. [1980] assumed R(i,j) to be 1.0.

The N(i,j) factors calculated for case A were obtained with a NO density profile which decreased by a factor of 7 from 31 km to 17 km. The preliminary (case A) retrieval, however, indicated a much smaller gradient in the NO profile, which is reflected in the smaller N(i,j) values calculated in case B for the layers below the balloon float altitude.

For the low Sun scans, 30 percent - 47 percent of the total NO column amount results from the layer above the balloon. Since NO is likely to be distributed non-uniformly at high altitudes, the N(i,j) values assumed for this layer are important in the retrieval. For cases A and B, they have been calculated with the profile from the steady-state photochemical model. Above 55 km, we assumed the shape of the reference profile of Frederick et. al. [1983]. The calculated values range from 1.0 to 1.21.

Recent in situ measurements of NO [Horvath et al., 1983] show considerable variability between 30 and 50 km at mid-latitudes, probably due to the action of transport processes. Our calculated N(i,j) factors for the layer above the balloon are, therefore, subject to an unknown amount of error. Because a high Sun scan of apparent angle θ and a low Sun scan of apparent angle $(180°-\theta)$ have identical ray geometries above the balloon float altitude, the uncertainty in the retrieval for a particular tangent height can be minimized by using an appropriate high Sun scan in the onion-peeling analysis. For the lower stratosphere where the NO concentrations are small (solar zenith angles of $\approx 94°$ for this experiment), the contribution to the total airmass from the path above the balloon float altitude is most important. Fortunately, the high-Sun scan available from this flight (85.85°) minimizes the uncertainties at these altitudes. In principle, N(i,j) factors for the layer above the balloon can be determined from measurements of average mixing ratios from a series of high Sun scans

covering a range of solar zenith angles. However, the NO lines are weak features in high Sun scans and measurement errors may make this procedure insufficiently precise.

Figure 2 shows the observed and least-squares best-fit spectra for the 1903.0-1907.0 cm^{-1} interval of the 85.85° scan. The observed and calculated spectra are plotted in the lower panel; at top are the residuals (observed-calculated), expressed as a percentage of the maximum observed amplitude in the interval. The standard deviation of the residuals is 1.32 percent. Arrows mark the locations of the four NO lines; their absorption is relatively weak. Most of the observed features in the high Sun scan are solar CO lines, which have broader widths than the atmospheric lines.

Figure 3 shows the results in the same region for the 93.36° scan (tangent altitude 22.3 km). The standard deviation of the residuals is 1.38 percent. The standard deviation of the residuals for the other scans range from 1.34 percent to 1.42 percent. For all the scans, the inclusion of parameters to model the sinusoidal modulation of the background caused by channel spectra was critical to obtain an accurate fit in the region of the NO lines.

Table IV compares the NO profile determined from the present study and the values derived from the same spectra by Blatherwick et al. [1980] with photochemical effects included in the analysis. The volume mixing ratios obtained in this work are 50-70 percent larger than retrieved by Blatherwick et al. [1980]. These differences are larger than can be accounted for by the different treatments of the photochemical effects. As can be seen from the fit to the background in figure 3, channel spectra occur in the NO spectral region, and it is possible that some of the differences in the retrieved profile result from the difficulty in defining the background for measurements with the equivalent width technique.

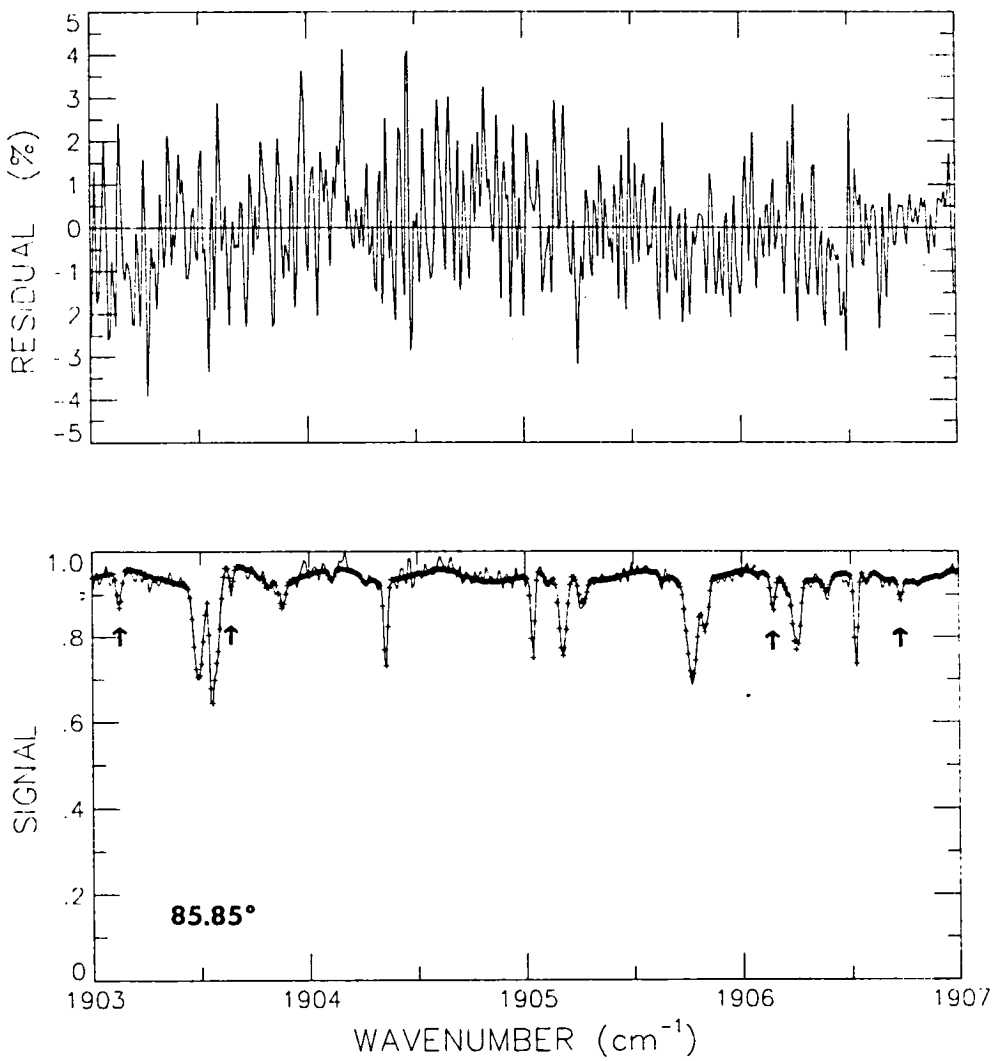

Fig. 2. Comparison of the 1903.0-1907.0-cm^{-1} region of a solar absorption spectrum (solid line) obtained at an astronomical zenith angle of 85.85^{o} and a least-squares best fit to the data. The arrows mark the locations of four NO absorption lines. Residuals expressed as a percentage of the maximum observed amplitude are shown in the upper panel.

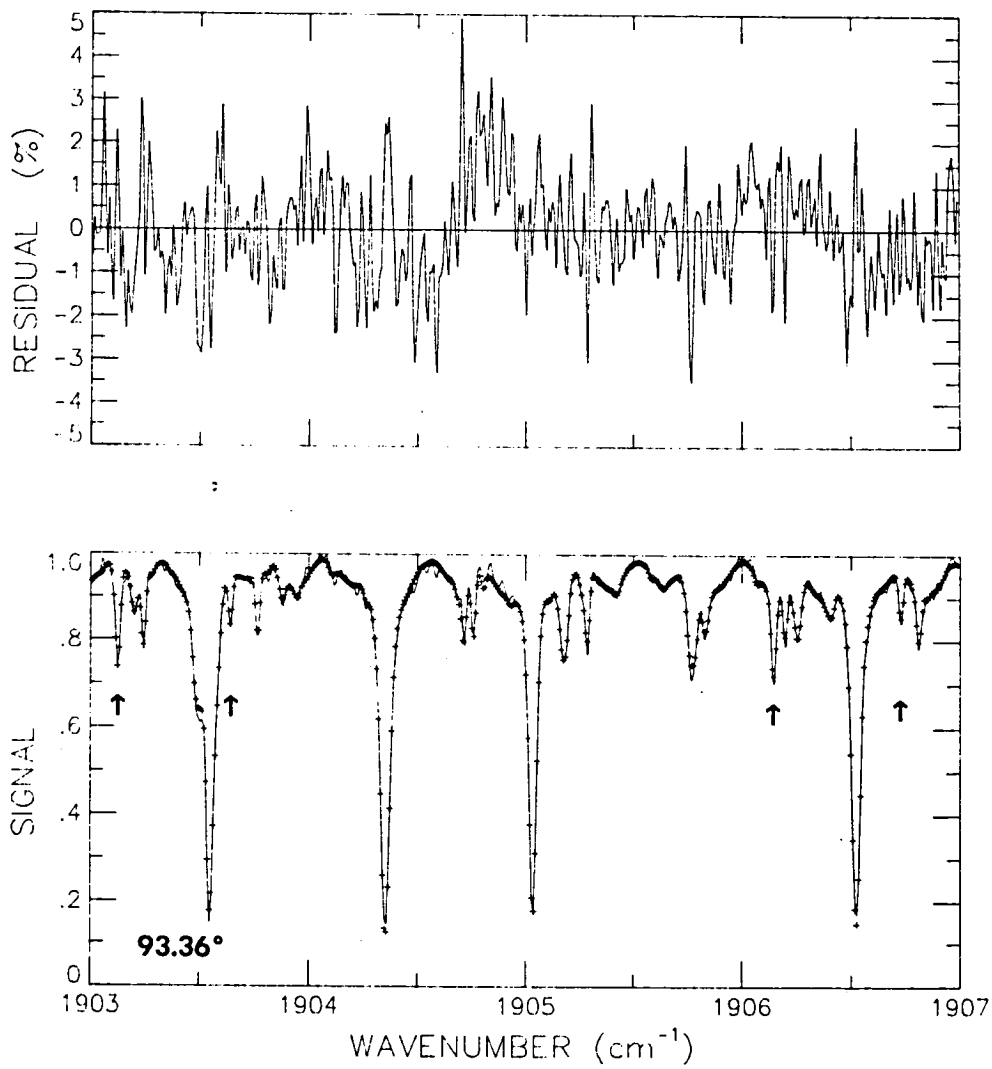

Fig. 3. Comparison of the 1903.0-1907.0-cm^{-1} region of a solar absorption spectrum (solid line) obtained at an astronomical zenith angle of 93.36^{o} (tangent altitude = 22.3 km) and a least-squares best fit to the data. The results are shown in the same format as Fig. 2.

Most of the published NO measurements were obtained in situ under high Sun conditions. Figure 4 compares our profile (converted from density to volume mixing ratio) and published in situ measurements for the same latitude and season. The measurements of Patel et al. [1974] were obtained with a spin flip Raman laser at 28 km on October 19, 1973. We have plotted their measured high Sun mixing ratio, which was obtained about 5 hours after visible sunrise. The other in situ data were derived from measurements made with chemiluminescence detectors. Loewenstein et al. [1978] reported NO concentrations as a function of latitude. The rectangles in figure 4 represent the range of their fall measurement near 33°N. Profiles derived from three flights in the fall of 1977 and 1978 by Ridley and Schiff [1981] are also plotted as are the measurements of M. McGhan and co-workers (as quoted by Ridley and Schiff, 1981).

Our values are about a factor of 2 lower than the in situ measurements presented in figure 4. This difference is expected since NO is rapidly converted to NO_2 near sunset. For example, the photochemical model calculations predict that the ratio of the sunset concentration to the concentration in the afternoon at a solar zenith angle of 45° is 0.56 at 17.5 km, 0.61 at 23.5 km, and 0.73 at 31.0 km. Clearly, quantitative comparisons between results obtained with absorption and in situ techniques will require simultaneous data.

Stratospheric NO profiles have been derived from solar absorption spectra recorded at sunset near 44°N [Ackerman et al., 1973; Ackerman et al., 1975; Louisnard et al., 1983]. These studies did not report the inclusion of diurnal corrections in the analysis. Our profile agrees very well with the results obtained in 1973 [Ackerman et al., 1973], but our values near 30 km are lower by ≈ 30 percent than the measurements determined

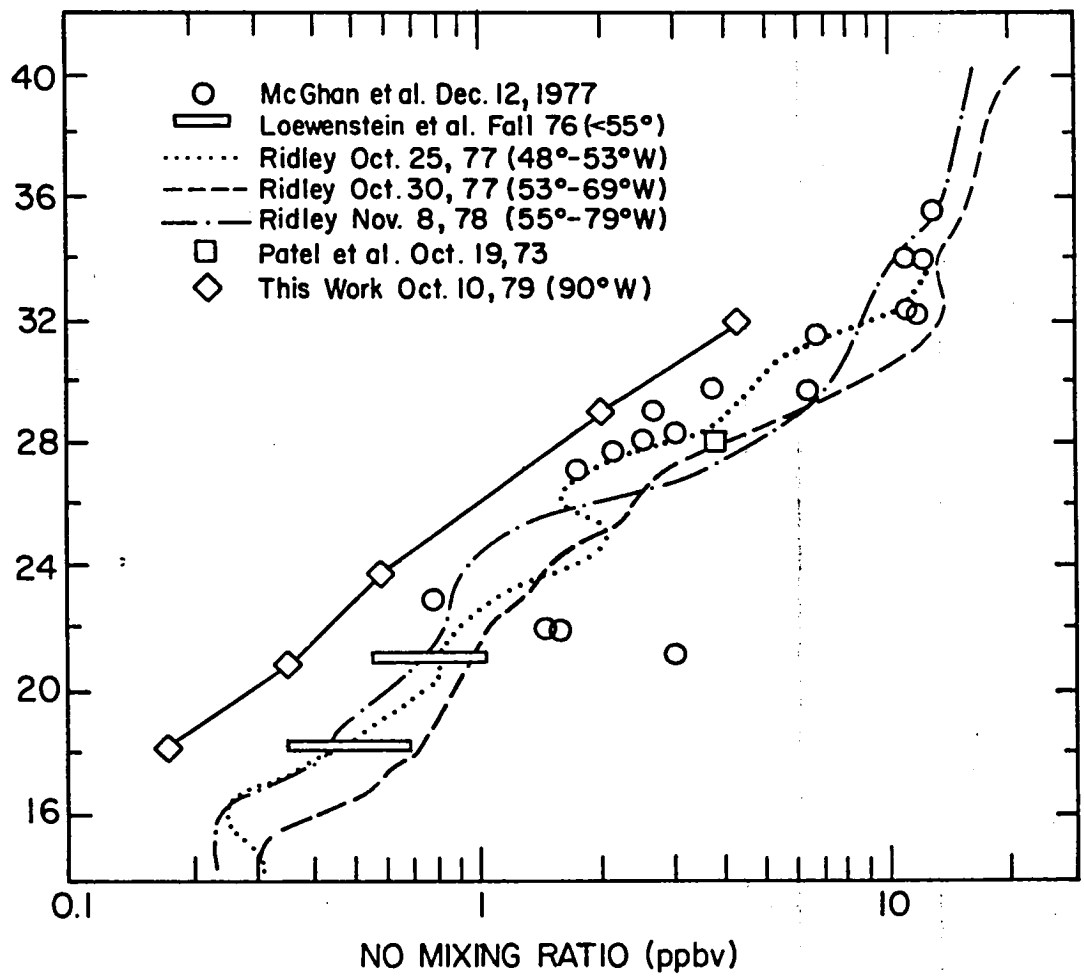

Fig. 4 Comparison for NO between the present sunset infrared absorption measurements and in situ measurements obtained for the same latitude and season under high Sun conditions.

from the other flight data [Ackerman et al., 1975; Louisnard et al., 1983]. Measurements obtained in September 1978 with a balloon-borne pressure modulator radiometer [Roscoe et al., 1981] show an average daytime profile which decreases more rapidly than both our sunset profile and the in situ data plotted in figure 4.

It needs to be emphasized that because the NO lines are weak features, high resolution is required for accurate quantitative measurements with the infrared absorption technique. Because the NO profile decreases rapidly below 30 km, inversion of the lower stratospheric portion of the profile is complicated not only by diurnal changes but also by the fact that very little of the NO absorption along the path originates from within the tangent layer. For example, for the path corresponding to the lowest Sun (94.14°) scan analyzed in this study, our profile indicates 77 percent of the NO molecules occur in layers above the tangent layer, so that small errors in fitting the NO lines will lead to large errors in the calculated tangent layer NO density. For these reasons, we estimate that the uncertainty in the NO profile increases from ≈20 percent at 32 km to ≈50 percent at 18 km. The uncertainties in the diurnal correction factors are not included in this estimate.

The many factors involved in the photochemical model calculations make it difficult to evaluate the accuracy of the diurnal correction factors. Recently, we compared ground-based measurements of the total vertical column amount of NO with values from our photochemical calculations [Rinsland et al., 1984c]. The measured column amounts were derived from an analysis of 0.01 cm^{-1} resolution infrared solar absorption spectra recorded near sunrise and sunset on February 23, 1981, at The National Solar Observatory

on Kitt Peak near Tucson, Arizona. The agreement obtained in this study between the measured and calculated diurnal changes is close to the estimated precision of the measurements (≈6 percent). However, it is important to note that the solar zenith angles of the scans studied were less than 86° so that the rapid changes expected for NO at sunrise and sunset were not observed. Measurements at a fixed altitude during sunrise and sunset, such as those reported by Ridley et al. [1977] and Ridley and Schiff [1981], provide the best test of photochemical model predictions.

Table V presents the CO_2 volume mixing ratio values obtained from the analysis of the two spectral regions. The effective altitude (H_{eff}) listed for each layer is the altitude corresponding to the airmass-weighted effective pressure along the path through the tangent layer. The value listed for the layer above the balloon float altitude is the altitude corresponding to the effective pressure of the high sun (85.85°) scan.

The absolute uncertainties in the CO_2 mixing ratios are estimated to be ≈ 15 percent based on the uncertainties in the experimental and spectroscopic parameters. At this level of accuracy, our results show no obvious trend in CO_2 mixing ratio with altitude. Within this uncertainty, they also agree with the more precise (±0.5 ppmv) gas-chromatographic measurements made in southern France (44°N) in 1979 [Volz et al., 1981]. This comparison suggests that systematic errors in the inversions arising from uncertainties in geometric factors (e.g., balloon float altitude, pointing angle) are likely to be relatively small for this data set. However, we note that a relatively large value of 386 ppmv was retrieved for the 22.3-27.4 km altitude region.

4.2 NO_2 Retrieval

The NO_2 profile has been derived from analysis of the 1602.0 - 1607.0 cm^{-1} interval (581 data points). Atmospheric lines of the ν_3 and the $\nu_2 + \nu_3 - \nu_2$ bands of NO_2, the ν_2 bands of H_2O, and the quadrupole fundamental vibration-rotation band of O_2 are seen in this range in addition to several relatively weak solar CO lines [Goldman et al., 1983]. The line structure is superimposed on broad absorption from the collision-induced fundamental band of O_2, which extends from $\approx$ 1400-1750 cm^{-1} [Rinsland et al., 1982b].

Improved positions and intensities for lines of the ν_3 and the $\nu_2 + \nu_3 - \nu_2$ bands of NO_2, derived recently from analysis of laboratory spectra recorded with the Kitt Peak Fourier transform interferometer, have been assumed in our analysis (R. A. Toth, JPL, private communication, 1983). For the NO_2 air-broadened half widths, an average value for N_2 broadening of 0.066 $cm^{-1}atm^{-1}$ at 296 K [Malathy Devi et al., 1982a] and a $T^{-0.968}$ temperature dependence [Malathy Devi et al., 1982b] have been assumed. Line parameters for H_2O and O_2 were taken from the 1982 AFGL major gas line parameters compliation [Rothman et al., 1983a], except for the positions of the stronger H_2O lines which were updated with the precise values measured by Guelachvili [1983]. No lines of CH_4 or N_2O have been identified within this interval in the stratospheric spectra [Goldman et al., 1983].

The same three cases used for the NO analysis were considered. Table VI presents the retrieved densities, and Table VII reports the correction factors. Essentially all of the NO_x above 40 km is in the form of NO [Solomon et al., 1982], so that in computing these factors it was

assumed that the NO_2 contribution above the upper altitude limit of our photochemical model calculations (55 km) is negligible. As expected, the diurnal corrections are much less important for deriving the profile of NO_2 than NO. The maximum difference in the values between the three cases is 15 percent for the lowest layer. Since $R(i,j) > 1$, diurnal corrections decrease the retrieved NO_2 densities. Despite the improvements in the accuracy of the line parameters and in the analysis procedure, the profile obtained in the present study differs only slightly from that retrieved from the same set of spectra by Niple et al. [1980]. An example of the fitting results is presented in figure 5, where the measured and least-squares best fit spectra are presented for the 93.36° scan. The standard deviations of the residuals for the six scans range from 1.1 percent to 2.0 percent of the peak intensity.

In figure 6 the results are compared with profiles derived at 33°N from long path infrared and visible absorption measurements at sunset by Murcray et al. [1974], Goldman et al. [1978], Borghi et al. [1983], and Kendall and Buijs [1983]. The present results are slightly lower than these published values. Average daytime mixing ratios derived from measurements with a pressure modulator radiometer near 32°N [Roscoe et al., 1981] are about a factor of 2 lower. We estimate that the uncertainty in our NO_2 profile increases from ≈ 20 percent at 32 km to ≈ 40 percent at 18 km.

5. Summary and Conclusions

We have reported simultaneous stratospheric sunset profiles of NO and NO_2 derived from solar absorption spectra using a nonlinear least squares spectral fitting technique and normalized diurnal correction factors calculated with a detailed time-dependent photochemical model. The NO

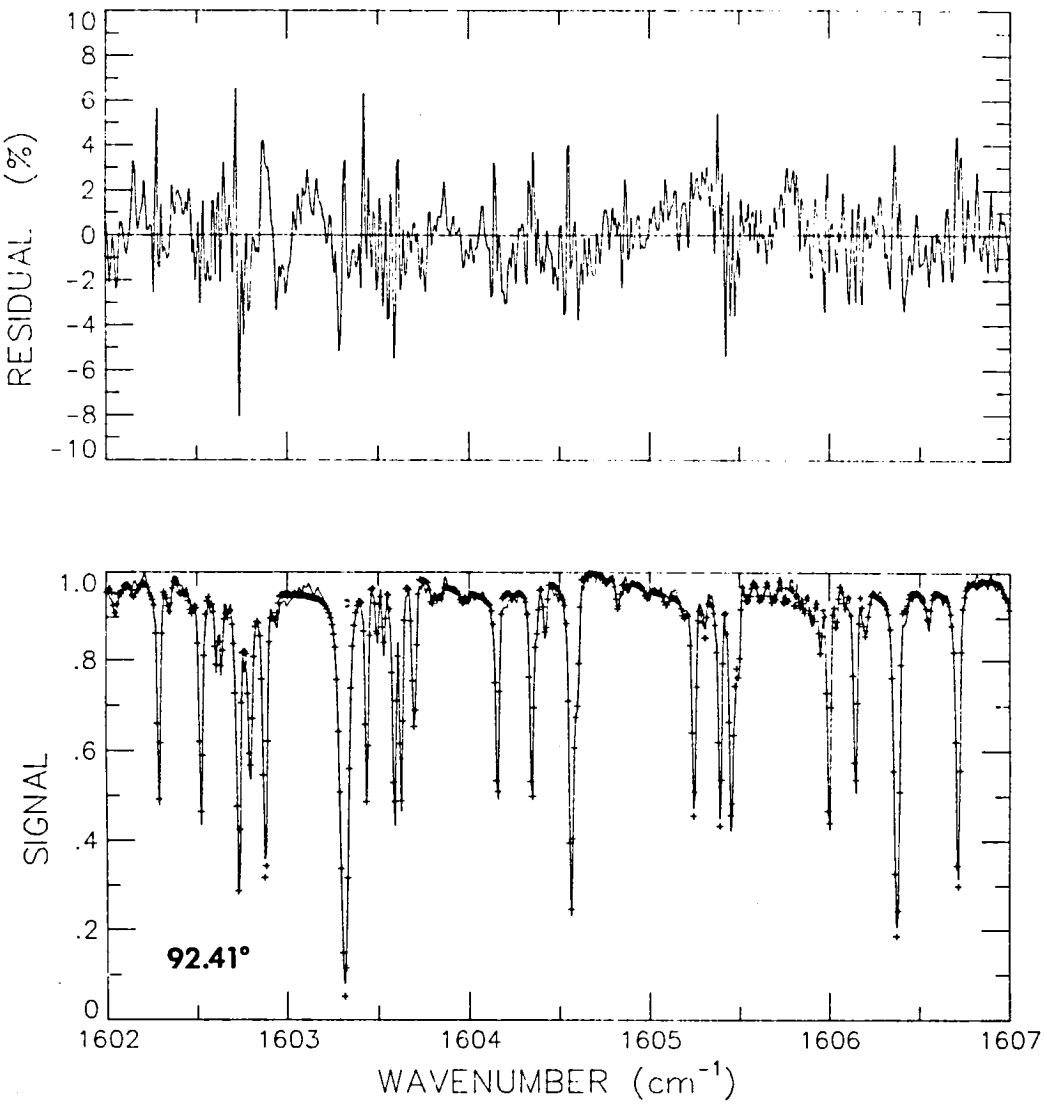

Fig. 5. Comparison of the 1602.0-1607.0-cm^{-1} region of a solar absorption spectrum obtained at an astronomical zenith angle of 92.41° (tangent altitude = 27.4 km) and a least-squares best fit to the data. The results are presented in the same format as Fig. 2 and Fig. 3.

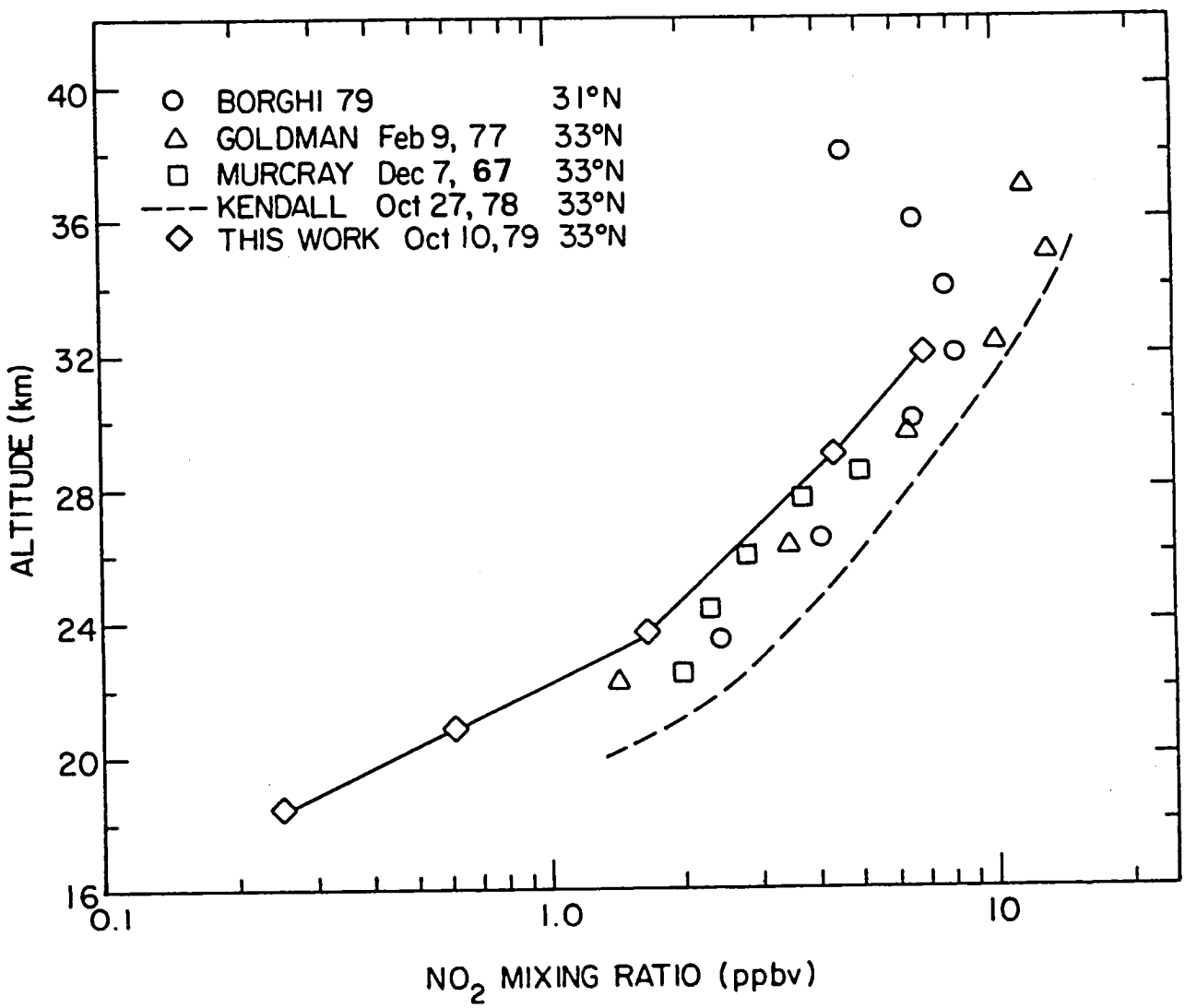

Fig. 6. Comparison of remote visible and infrared measurements of the NO_2 sunset profile at 31^{o}-33^{o}N.

densities obtained from the analysis are about a factor of 2 lower than published values obtained in situ under high Sun conditions during the same season and at the same latitude. This difference is consistent with the expected rapid decay of NO into NO_2 at sunset. The NO_2 measurements are slightly lower than values determined previously from solar absorption spectra recorded at sunset near 33°N. As a check for systematic errors in the analysis, the CO_2 profile has also been retrieved. These results are in good agreement with precise in situ measurements of CO_2 in the mid-stratosphere [Volz et al., 1981]. The NO and NO_2 profiles reported here in combination with the simultaneous profiles of HNO_3, H_2O, CH_4, O_3, and N_2O reported previously [Goldman et al., 1980; Rinsland et al., 1982a; Rinsland et al., 1984a] represent a consistent set of measurements useful for comparisons with profiles calculated by models of stratospheric chemistry.

Our results are in agreement with previous studies [Kerr et al., 1977; Murcray et al., 1978; Boughner et al., 1980] which show that diurnal corrections for NO are important for solar occultation measurements only for altitudes below about 30 km and that diurnal corrections produce only a relatively small change in the results for NO above 30 km and for NO_2 at all altitudes. Normalized factors calculated with the procedure described in this report should also prove useful for improving the accuracy of the retrievals of the profiles of diurnally varying gases from satellite measurements, such as will be obtained by ATMOS and HALOE. Our calculations indicate that normalized diurnal correction factors are relatively insensitive to changes in a number of model input parameters so that reasonably precise results can be derived without detailed knowledge of the profiles of the chemically-connected species, temperature, and pressure.

However, much further work needs to be done to access the absolute accuracies of the diurnal variations of NO and NO_2 calculated by current photochemical models. Additional diurnal measurements of these species with simultaneous O_3 and temperature data are needed, particularly with sufficient time resolution to study the rapid changes in concentration at sunrise and sunset.

References

Ackerman, M., D. Frimout, C. Muller, D. Nevejans, J.-C. Fontanella, A. Girard, and N. Louisnard, Stratospheric nitric oxide from infrared spectra, Nature, 245, 205-206, 1973.

Ackerman, M., J. C. Fontanella, D. Frimout, A. Girard, N. Louisnard, and C. Muller, Simultaneous measurements of NO and NO_2 in the stratosphere, Planet. Space Sci., 23, 651-660, 1975.

Amiot, C., and G. Guelachvili, Extension of the 10^6 samples Fourier spectrometry to the Indium Antimonide region: Vibration-rotation bands of $^{14}N_2{}^{16}O$: 3.3 - 5.5 μm region, J. Mol. Spectrosc., 59, 171-190, 1976.

Blatherwick, R. D., A. Goldman, D. G. Murcray, F. J. Murcray, G. R. Cook, and J. W. Van Allen, Simultaneous stratospheric mixing ratio profiles of NO and NO_2 as derived from balloon-borne infrared solar spectra, Geophys. Res. Lett., 7, 471-473, 1980.

Borghi, R., D. Cariolle, A. Girard, J. Laurent, and N. Louisnard, Comparaison entre les resultats d'un modele unidimensionnel et des resultats de mesures stratospheriques de CH_4, H_2O et des oxydes d'azote, Revue Phys. Appl., 18, 229-237, 1983.

Boughner, R., J. C. Larsen, and M. Natarajan, The influence of NO and CℓO variations at twilight on the interpretation of solar occultation measurements, Geophys. Res. Lett., 7, 231-234, 1980.

Callis, L. B., M. Natarajan, and R. E. Boughner, On the relationship between the greenhouse effect, atmospheric photochemistry, and species distribution, J. Geophys. Res., 88, 1401-1426, 1983.

References (continued)

Chang, Y. S., J. H. Shaw, J. G. Calvert, and W. M. Uselman, Determination of abundances of gases from solar spectra, J. Quant. Spectrosc. Radiat. Transfer, 19, 599-605, 1978.

Flaud, J. M., C. Camy-Peyret, and R. A. Toth, Water vapour line parameters from microwave to medium infrared, Pergamon, Oxford, 1981.

Frederick, J. E., R. B. Abrams, and P. J. Crutzen, The Delta band dissociation of nitric oxide: A potential mechanism for coupling thermospheric variations to the mesosphere and stratosphere, J. Geophys. Res., 88, 3829-3835, 1983.

Gallery, W. O., F. X. Kneizys, and S. A. Clough, Air mass computer program for atmospheric transmittance/radiance calculation: FSCATM, AFGL-TR-83-0065, Air Force Geophysics Lab, Bedford, MA, 1983.

Gillis, J. R., and A. Goldman, Nitric oxide IR line parameters for the upper atmosphere, Appl. Opt., 21, 1161-1163, 1982.

Goldman, A., and R. S. Saunders, Analysis of atmospheric infrared spectra for altitude distribution of atmospheric trace constituents-I. Method of analysis, J. Quant. Spectrosc. Radiat. Transfer, 21, 155-161, 1979.

Goldman, A., F. G. Fernald, W. J. Williams, and D. G. Murcray, Vertical distribution of NO_2 in the stratosphere as determined from balloon measurements of solar spectra in the 4500A region, Geophys. Res. Lett., 5, 257-260, 1978.

Goldman, A., D. G. Murcray, F. J. Murcray, and E. Niple, High resolution IR balloon-borne solar spectra and laboratory spectra in the HNO_3 1720-cm^{-1} region: an analysis, Appl. Opt., 19, 3721-3724, 1980.

References (continued)

Goldman, A., R. D. Blatherwick, F. J. Murcray, J. W. Van Allen, F. H. Murcray and D. G. Murcray, New atlas of stratospheric IR absorption spectra, Vol. I, Line positions and identifications, Vol. II, The spectra, Department of Physics, University of Denver, 1983.

Guelachvili, G., Experimental Doppler-limited spectra of the ν_2 bands of $H_2{}^{16}O$, $H_2{}^{17}O$, $H_2{}^{18}O$ and HDO by Fourier transform spectroscopy. Secondary wavenumber standards between 1066 and 2296 cm^{-1}, J. Opt. Soc. Amer., 73, 137-150, 1983.

Guelachvili, G., D. De Villeneuve, R. Farrenq, W. Urban, and J. Verges, Dunham coefficients for seven isotopic species of CO, J. Mol. Spectrosc., 98, 64-79, 1983.

Horvath, J. J., J. E. Frederick, N. Orsini, and A. R. Douglass, Nitric oxide in the upper stratosphere: Measurements and geophysical interpretation, J. Geophys. Res., 88, 10809-10817, 1983.

Kendall, D. J. W., and H. L. Buijs, Stratospheric NO_2 and upper limits of $CH_3C\ell$ and C_2H_6 from measurements at 3.4 μm, Nature, 303, 221-222, 1983.

Kerr, J. B., W. F. J. Evans, and J. C. McConnell, The effects of NO_2 changes at twilight on tangent ray NO_2 measurements, Geophys. Res. Lett., 4, 577-579, 1977.

Kilston, S., N-type carbon stars and the 3-α process, Pub. Astron. Soc. Pacific, 87, 189-206, 1975.

Kyle, T. G., and R. Blatherwick, Smearing of interferograms in Fourier transform spectroscopy, Appl. Opt., 23, 261-263, 1984.

References (continued)

Larsen, J. C., and R. E. Boughner, The feasibility of using time-dependent photochemical calculations to infer radical species concentrations from solar occultation absorption measurements, in Proc. Quadrennial Int. Ozone Symp., Vol. II, edited by J. London, pp. 948-955, IAMAP, Boulder, CO, 1981.

Loewenstein, M., W. L. Starr, and D. G. Murcray, Stratospheric NO and HNO_3 observations in the Northern Hemisphere for three seasons, Geophys. Res. Lett., 5, 531-534, 1978.

Louisnard, N., G. Fergant, A. Girard, L. Gramont, O. Lado-Bordowsky, J. Laurent, S. Le Boiteux, and M. P. Lemaitre, Infrared absorption spectroscopy applied to stratospheric profiles of minor constituents, J. Geophys. Res. Lett., 88, 5365-5376, 1983.

Maier, E. J., A. C. Aikin, and J. E. Ainsworth, Stratospheric nitric oxide and ozone measurements using photoionization mass spectrometry and UV absorption, Geophys. Res. Lett., 5, 37-40, 1978.

Malathy Devi, V., B. Fridovich, G. D. Jones, D. G. S. Snyder, P. P. Das, J. M. Flaud, C. Camy-Peyret, and K. Narahari Rao, Tunable diode laser spectroscopy of NO_2 at 6.2 μm, J. Mol. Spectrosc., 93, 179-195, 1982a.

Malathy Devi, V., B. Fridovich, G. D. Jones, D. G. S. Snyder, and A. Neuendorffer, Temperature dependence of the widths of N_2-broadened lines of the ν_3 band of $^{14}N^{16}O_2$, Appl. Opt., 21, 1537-1538, 1982b.

Mihelcic, D., D. H. Ehhalt, G. F. Kulessa, J. Klomfass, M. Trainer, U. Schmidt, and H. Rohrs, Measurements of free radicals in the atmosphere by matrix isolation and electron paramagnetic resonance, Pure Appl. Geophys., 116, 530-536, 1978.

References (continued)

Morse, P. G., Progress report on the ATMOS sensor: Design description and development status, AIAA Sensor Systems for the 80's Conference, Colorado Springs, CO, Technical paper 80-1914-CP (1980).

Murcray, D. G., A. Goldman, W. J. Williams, F. H. Murcray, J. N. Brooks, J. Van Allen, R. N. Stocker, J. J. Kosters, D. B. Barker, and D. E. Snider, Recent results of stratospheric trace-gas measurements from balloon-borne spectrometers, Proc. Third CIAP Conf., A. J. Broderick and T. M. Hard, editors, DOT-TSC-OST-74-15, U. S. Dept. of Transportation, Washington, D.C., pp. 184-192, 1974.

Murcray, D. G., A. Goldman, G. R. Cook, D. K. Rolens, and L. R. Megill, On the interpretation of infrared solar spectra for altitude distribution of atmospheric trace constituents, U. S. Dept. of Transportation Report No. FAA-EE-78-30, 1978.

Niple, E., Nonlinear least squares analysis of atmospheric absorption spectra, Appl. Opt., 19, 3481-3490, 1980.

Niple, E., W. G. Mankin, A. Goldman, D. G. Murcray, and F. J. Murcray, Stratospheric NO_2 and H_2O mixing ratio profiles from high resolution infrared solar spectra using nonlinear least squares, Geophys. Res. Lett., 7, 489-492, 1980.

Park, J. H., Effect of interferogram smearing on atmospheric limb sounding by Fourier transform spectroscopy, Appl. Opt., 21, 1356-1366, 1982.

Park, J. H., Analysis method for Fourier transform spectroscopy, Appl. Opt., 22, 835-849, 1983.

References (continued)

Patel, C. K. N., E. G. Burkhardt, and C. A. Lambert, Spectroscopic measurements of stratospheric Nitric oxide and water vapor, Science, 184, 1173-1176, 1974.

Ridley, B. A., and H. I. Schiff, Stratospheric odd nitrogen: Nitric oxide measurements at 32°N in autumn, J. Geophys. Res., 86, 3167-3172, 1981.

Ridley, B. A., M. McFarland, J. T. Bruin, H. I. Schiff, and J. C. McConnell, Sunrise measurements of stratospheric nitric oxide, Can. J. Phys., 55, 212-221, 1977.

Rinsland, C. P., A. Goldman, F. J. Murcray, D. G. Murcray, M. A. H. Smith, R. K. Seals, Jr., J. C. Larsen, and P. L. Rinsland, Stratospheric N_2O mixing ratio profile from high-resolution balloon-borne solar absorption spectra and laboratory spectra near 1880 cm^{-1}, Appl. Opt., 21, 4351-4355, 1982a.

Rinsland, C. P., M. A. H. Smith, R. K. Seals, Jr., A. Goldman, F. J. Murcray D. G. Murcray, J. C. Larsen, and P. L. Rarig, Stratospheric measurements of collision-induced absorption by molecular oxygen, J. Geophys. Res., 87, 3119-3122, 1982b.

Rinsland, C. P., A. Goldman, F. J. Murcray, D. G. Murcray, M. A. H. Smith, R. K. Seals, Jr., J. C. Larsen, and P. L. Rinsland, Stratospheric temperature profile from balloon-borne measurements of the 10.4-μm band of CO_2, J. Quant. Spectrosc. Radiat. Transfer, 30, 327-334, 1983a.

Rinsland, C. P., D. C. Benner, D. J. Richardson, and M. A. H. Smith, Line parameters for the 5-μm bands of carbon dioxide, presented at Thirty-Eighth Symposium on Molecular Spectroscopy, Ohio State University, Columbus, OH, paper ME6, 1983b.

References (continued)

Rinsland, C. P., D. Chris Benner, D. J. Richardson, and R. A. Toth, Absolute intensity measurements of the $(11^10)_{II} \leftarrow 00^00$ band of $^{12}C^{16}O_2$ at 5.2 μm, Appl. Opt., 23, 3805-3809, 1983c.

Rinsland, C. P., A. Goldman, V. Malathy Devi, B. Fridovich, D. G. S. Snyder, G. D. Jones, F. J. Murcray, D. G. Murcray, M. A. H. Smith, R. K. Seals, Jr., M. T. Coffey, and W. G. Mankin, Simultaneous stratospheric measurements of H_2O, HDO, and CH_4 from balloon-borne and aircraft infrared solar absorption spectra and tunable diode laser laboratory spectra of HDO, J. Geophys. Res., in press, 1984a.

Rinsland, C. P., D. C. Benner, V. Malathy Devi, P. S. Ferry, C. H. Sutton, and D. J. Richardson, Atlas of high resolution infrared spectra of carbon dioxide: February 1984 edition, NASA Technical Memorandum 85764, NASA Langley Research Center, Hampton, VA, 467 pp., 1984b.

Rinsland, C. P., R. E. Boughner, J. C. Larsen, G. M. Stokes, and J. W. Brault, Diurnal variations of atmospheric nitric oxide: Ground-based infrared spectroscopic measurements and their interpretation with time-dependent photochemical model calculations, J. Geophys. Res., in press, 1984c.

Roscoe, H. K., J. R. Drummond, and R. F. Jarnot, Infrared measurements of stratospheric composition. III. The daytime changes of NO and NO_2, Proc. R. Soc. London, A375, 507-528, 1981.

Rothman, L. S., R. R. Gamache, A. Barbe, A. Goldman, J. R. Gillis, L. R. Brown, R. A. Toth, J.-M. Flaud, and C. Camy-Peyret, AFGL atmospheric absorption line parameters compilation: 1982 edition, Appl. Opt., 22, 2247-2256, 1983a.

References (concluded)

Rothman, L. S., A. Goldman, J. R. Gillis, R. R. Gamache, H. M. Pickett, R. L. Poynter, N. Husson, and A. Chedin, AFGL trace gas compilation: 1982 version, Appl. Opt., 22, 1616-1627, 1983b.

Russell, J. M., J. H. Park, and S. R. Drayson, Global monitoring of stratospheric halogen compounds from a satellite using gas filter spectroscopy in the solar occultation mode, Appl. Opt., 16, 607-612, 1977.

Solomon, S., P. J. Crutzen, and R. G. Roble, Photochemical coupling between the thermosphere and the lower atmosphere 1. Odd nitrogen from 50 to 120 km, J. Geophy. Res., 87, 7206-7220, 1982.

Toth, R. A., Temperature sounding from the absorption spectrum of CO_2 at 4.3 μm, Appl. Opt., 16, 2661-2668, 1977.

Toth, R. A., and C. B. Farmer, Line strengths of H_2O and N_2O in the 1900 cm^{-1} region, J. Mol. Spectrosc., 55, 182-191, 1975.

Volz, A., D. H. Ehhalt, A. Khedim, U. Schmidt, W. Borchers, and P. Fabian, Vertical profiles of CO_2 in the stratosphere, in Proc. Quadrennial Int. Ozone Symp., Vol. II, edited by J. London, pp. 824-828, IAMAP, Boulder, CO, 1981.

Table I. Profile Results for NO

Layer Boundaries (km)	NO Sunset Density (10^8 cm^{-3})		
	No Corrections (R=N=1)	Case A Corrections	Case B Corrections
33.0-100.0	(3.4)	(3.4)	(3.4)
31.4- 33.0	14.8	13.2	13.1
27.4- 31.4	9.1	9.6	9.5
22.3- 27.4	4.5	6.0	6.2
19.7- 22.3	3.8	5.2	5.7
17.3- 19.7	2.7	4.5	4.7

Values for the layer above the balloon (33.0-100 km) are enclosed in parentheses to denote their larger uncertainty.

Table II. Correction Factors for the NO Inversion

Layer Boundaries (km)	Scan (°)	R(i,j)		N(i,j)	
		Case A	Case B	Case A	Case B
33.0-100.0	85.85	1.0	1.0	1.0	1.0
	91.30	1.0	1.0	1.21	1.21
	92.41	1.0	1.0	1.12	1.12
	93.36	1.0	1.0	1.05	1.05
	93.78	1.0	1.0	1.03	1.03
	94.14	1.0	1.0	1.01	1.01
31.4- 33.0	91.30	0.98	0.98	1.0	1.0
	92.41	0.87	0.90	1.03	0.995
	93.36	0.71	0.70	1.03	0.996
	93.78	0.66	0.66	1.03	0.996
	94.14	0.63	0.64	1.03	0.996
27.4- 31.4	92.41	0.95	0.95	1.0	1.0
	93.36	0.74	0.76	1.09	1.02
	93.78	0.67	0.67	1.09	1.02
	94.14	0.64	0.64	1.10	1.02
22.3- 27.4	93.36	0.89	0.89	1.0	1.0
	93.78	0.78	0.79	1.12	1.04
	94.14	0.72	0.73	1.14	1.04
19.7- 22.3	93.78	0.92	0.91	1.0	1.0
	94.14	0.84	0.82	1.03	1.03
17.3- 19.7	94.14	0.93	0.93	1.0	1.0

Table III. Comparison for NO between the Case B Diurnal Correction Factors and the Values Estimated by Blatherwick et al. [1980].

Layer Boundaries (km)	Scan (°)	Diurnal Correction Factor R(i,j)	
		Case B (This Study)	Blatherwick et al. [1980]
33.0-100.0	85.85	1.0	1.0
	91.30	1.0	1.0
	92.41	1.0	1.0
	93.36	1.0	1.0
	93.78	1.0	1.0
	94.14	1.0	1.0
31.4- 33.0	91.30	0.98	1.0
	92.41	0.90	0.75
	93.36	0.70	0.50
	93.78	0.66	0.50
	94.14	0.64	0.50
27.4- 31.4	92.41	0.95	1.0
	93.36	0.76	0.50
	93.78	0.67	0.50
	94.14	0.64	0.50
22.3- 27.4	93.36	0.89	1.0
	93.78	0.79	0.50
	94.14	0.73	0.50
19.7- 22.3	93.78	0.91	1.0
	94.14	0.82	0.50
17.3- 19.7	94.14	0.93	1.0

Table IV. Comparison for NO Between the Case B Sunset Profile Derived in this Study and the Profile Determined by Blatherwick et al. [1980]

Layer Boundaries (km)	NO Sunset Volume Mixing Ratio (ppbv)	
	Case B (This Study)	Blatherwick et al. [1980]
33.0-100.0	9.36	6.35
31.4- 33.0	4.40	3.04
27.4- 31.4	1.95	1.28
22.3- 27.4	0.59	0.32
19.7- 22.3	0.31	0.19
17.3- 19.7	0.17	0.098

The values of Blatherwick et al. [1980] correspond to the results obtained with photochemical effects included in the analysis.

Table V. CO_2 Volume Mixing Ratio β Obtained from Analysis of Two Spectral Intervals

Layer (km)	H_{eff} (km)	CO_2 Mixing Ratios for Spectral Range		Average Value
		1903.0-1907.0 cm^{-1}	1911.95-1917.0 cm^{-1}	
		β(ppmv)	β(ppmv)	β(ppmv)
33.0-100.0	37.5	318	299	308
31.4- 33.0	31.9	350	345	347
27.4- 31.4	28.5	304	341	323
22.3- 27.4	23.5	387	385	386
19.7- 22.3	20.4	306	328	317
17.3- 19.7	18.0	317	340	328

Table VI. Profile Results for NO_2

Layer Boundaries (km)	NO_2 Sunset Density (10^9 cm^{-3})		
	No Corrections (R=N=1)	Case A Corrections	Case B Corrections
33.0-100.0	(0.17)	(0.17)	(0.17)
31.4- 33.0	2.3	2.1	2.0
27.4- 31-4	2.2	2.1	2.1
22.3- 27.4	2.0	1.8	1.7
19.7- 22.3	1.1	1.0	1.1
17.3- 19.7	0.81	0.68	0.68

Values for the layer above the balloon (33.0-100.0 km) are enclosed in parentheses to denote their larger uncertainty.

Table VII. Correction Factors for the NO_2 Inversion

Layer Boundaries (km)	Scan (°)	R(i,j)		N(i,j)	
		Case A	Case B	Case A	Case B
33.0-100.0	85.85	1.0	1.0	1.0	1.0
	91.30	1.0	1.0	1.58	1.58
	92.41	1.0	1.0	1.26	1.26
	93.36	1.0	1.0	1.10	1.10
	93.78	1.0	1.0	1.06	1.06
	94.14	1.0	1.0	1.02	1.02
31.4- 33.0	91.30	1.01	1.02	1.0	1.0
	92.41	1.06	1.06	1.00	0.971
	93.36	1.14	1.18	1.00	0.969
	93.78	1.16	1.20	1.00	0.969
	94.14	1.17	1.21	1.01	0.969
27.4- 31.4	92.41	1.02	1.03	1.0	1.0
	93.36	1.10	1.12	1.01	0.998
	93.78	1.12	1.16	1.02	0.999
	94.14	1.12	1.17	1.02	1.00
22.3- 27.4	93.36	1.03	1.10	1.0	1.0
	93.78	1.06	1.09	1.10	1.02
	94.14	1.07	1.12	1.11	1.02
19.7- 22.3	93.78	1.02	1.04	1.0	1.0
	94.14	1.04	1.08	1.05	1.06
17.3- 19.7	94.14	1.03	1.06	1.0	1.0

1. Report No.	2. Government Accession No.	3. Recipient's Catalog No.
NASA TM-86285		

4. Title and Subtitle	5. Report Date
Stratospheric NO and NO_2 Profiles at Sunset from Analysis of High-Resolution Balloon-borne Infrared Solar Absorption Spectra obtained at 33°N and Calculations with a Time-Dependent Photochemical Model	August 1984
	6. Performing Organization Code 147-44-02-70
7. Author(s) C. P. Rinsland, R. E. Boughner, J. C. Larsen*, A. Goldman**, F. J. Murcray**, and D. G. Murcray**	8. Performing Organization Report No.
	10. Work Unit No.
9. Performing Organization Name and Address NASA Langley Research Center Hampton, VA 23665	11. Contract or Grant No.
	13. Type of Report and Period Covered Technical Memorandum
12. Sponsoring Agency Name and Address National Aeronautics and Space Administration Washington, D. C. 20546	14. Sponsoring Agency Code

15. Supplementary Notes

* Systems and Applied Sciences Corporation
Hampton, VA 23665

** University of Denver
Denver, CO 80208

16. Abstract

Simultaneous stratospheric vertical profiles of NO and NO_2 at sunset have been derived from an analysis of 0.02-cm^{-1} resolution infrared solar absorption spectra recorded from a float altitude of 33 km with the University of Denver interferometer system during a balloon flight from Alamogordo, N.M., near 33°N on October 10, 1979. A nonlinear least squares procedure has been used to analyze the spectral data in regions of absorption by NO and NO_2 lines. Normalized factors, determined from calculations of time-dependent altitude profiles with a detailed photochemical model, have been included in the onion-peeling analysis to correct for the rapid diurnal changes in NO and NO_2 concentrations with time near sunset. The CO_2 profile has also been derived from the analysis and is reported.

17. Key Words (Suggested by Author(s))	18. Distribution Statement
Remote sensing Atmospheric optics Infrared spectra Atmospheric gases Nitric oxide	Unclassified -- Unlimited Subject catagory 46

19. Security Classif. (of this report)	20. Security Classif. (of this page)	21. No. of Pages	22. Price
Unclassified	Unclassified	45	A03

For sale by the National Technical Information Service, Springfield, Virginia 22161